İstanbul Yerbilimleri Dergisi, C.25, S.2, SS. 85-103, Y. 2012

GEOCHEMICAL AND MINERALOGICAL RELATIONSHIPS BETWEEN MANGANESE SILICATE MINERALS AND ZINC ORE MINERALIZATION AT GÜRECE CONTACT AUREOLE (BIGA PENINSULA, NW-TURKEY)

GÜRECE KONTAKT ZONUNDA (BİGA YARIMADASI, KB TÜRKİYE) MANGAN SİLİKAT MİNERALLERİ VE ÇİNKO CEVHER MİNERALİZASYONU ARASINDA JEOKİMYASAL VE MİNERALOJİK İLİŞKİLER

Sinan Öngen*, Namık Aysal, Direnç Azaz

İ.Ü. Mühendislik Fakültesi Jeoloji Mühendisliği Bölümü, 34320, Avcılar – İstanbul

ongens@istanbul.edu.tr

ABSTRACT

In this study, we show the diversity of bimetasomatic skarn mineralisation and associated zinc ore formation. At Bakırlık Tepe hill we observed in a roof pendant contact metamorphosed units of the Çetmi Mélange bordering the monzonitic Gürece Pluton of Eocene age. Additionally, two types of endoskarn were identified in this zone; diopside-bearing monzonite along the garnet skarn and hedenbergite-bearing monzogabbro along the pyroxene skarn contacts. The ratio of garnet skarn/pyroxene skarn is about 2:1. The presence of manganiferous minerals (johannsenite, Mn-garnet, Mn-chlorite) in the pyroxene skarn provides evidence for sphalerite mineralization at temperatures less than 400°C, under high oxygen fugacity and in the presence of water-enriched fluids.

Key words: Biga Peninsula, Gürece pluton, Mn-skarn, sphalerite ore.

ÖZ

Bu çalışmada, bimetasomatik skarn mineralizasyonu ve buna bağlı çinko cevherleşmesinin ilişkisi gösterilmektedir. Bakırlık Tepe'de Eosen yaşlı Gürece monzonitik plutonu dokanağında gözlenen asılı tavan bölümünde Çetmi Melanjına ait birimlerde kontak metamorfizma olayı gözlenmiştir. Bu zonda ayrıca, iki tür endoskarn da gelişmiştir: granatlı skarn dokanağında diyopsidli monzonit, piroksenli skarn dokanağında hedenberjitli monzogabbro. Mineral birlikteliği olarak granat skarn/piroksen skarn oranı 2:1 gibidir. Piroksenli skarn içinde manganezli minerallerin (johansenit, Mn-granat, Mn-klorit) bulunuşu 400 °C'den düşük sıcaklık, yüksek oksijen fugasitesi ve su içerikli akışkanların varlığı koşullarında sfalerit mineralozisyonunu sağlamıştır.

Anahtar kelimeler: Biga Yarımadası, Gürece Plutonu, Mn-skarn, sfalerit cevheri.

1. INTRODUCTION

Mn-skarns were commonly considered specific part of the calcic skarns but recently their characters were re-defined as follows:

- The most striking difference of Mn-skarns is the very high value of the (Mn+Fe)/Mg ratio in silicate minerals (Mn-hedenbergite, Mn-salite, spessartine, rhodonite, bustamite, Mn-ilvaite, Mn-actinolite, Mn-chlorite) and the predominance of pyroxene skarn relative to garnet skarn (Einaudi and Burt, 1982; Meinert, 1992; Meinert et al. 2005).

- The Mn-skarn typically forms after the Ca-skarn replacement. It is characterized by infiltration metasomatism and occurs far from the magmatic contact ("distal skarn"; Kerrick, 1977). Several examples in the world show considerable amounts of Zn-Pb ores, not only in the skarn but also in the limestone outside the aureole, indicating that the mineralization may develop outside the stability field of common calc-silicate minerals (Zharikov, 1970 Burt, 1977; Meinert, 1992; Meinert et al. 2005).

- The estimated temperatures of Mn-skarn are lower than those of Ca-skarn. Studies on fluid inclusions gave values of the order of 200-450°C, while for the Ca-skarn, they are higher (i.e. 400-650°C; Burton et al., 1982).

- The mineralized Mn-skarn always contains Pb-Zn (Ag) minerals like sphalerite, galenite, pyrite, chalcopyrite, magnetite and silver sulfides. Ore mineralization in Ca-skarns, on the other hand, is extremely varied, including Fe, Cu, Pb, Zn, W, Sn, Mo, Bi, Au ores (Megaw et al, 1988).

- The Mn-skarns are absent from the Paleozoic and Precambrian terrains. The majority of Mesozoic or more recent intrusions associated with Mn-skarns have a monzonitic-granitic composition (Yiming, 1991).

In Ca-skarns, increasing temperatures and/or decreasing XCO_2 values facilitate the crystallization of calc-silicate minerals (Greenwood, 1967). Formation of calc-silicate minerals may start at lowest temperatures in water enriched fluids.

Currently, one of the most typical examples of manganiferous Zn-skarn minerals occurs in Gürece village (province of Çanakkale, NW Turkey). The Gürece skarns have a bimetasomatic character (according to the definition of Korzhinskii, 1970). NE of Gürece, on Bakırlık Tepe hill, the duality of skarn (garnet and pyroxene skarns) and associated metal mineralization are exposed. An old quarry on the top of the hill indicates an operation of 300 tons of sphalerite and chalcopyrite ore (Brennich, 1961). On the site, only the marble is currently being operated. At about 150 meters east of the Bakırlık Tepe hill, a body of magnetite, 3 meters thick and 50 meters long, crops out between the garnet skarn and marble. Description of manganesiferous skarns near Gürece allows us to establish the relationship with the zinc mineralization (Öngen, 1992).

2. GEOLOGICAL CONTEXT

Belonging to the northern part of the Çamlıca Metamorphic Complex (ÇMC) and/or the Kemer Metamorphic Complex (KMC), a sheat of high pressure rocks of continental crustal origin of Late Cretaceous age occur in the Rhodope - Istranca Zone (Fig. 1; Aygül et al, 2012). This complex is composed mainly of mica schists, calc-schists and marble with minor metabasite and serpentinite. Main difference between the ÇMC and KMC is that the latter does not contain eclogite slivers (Beccaletto et al, 2007). Metamorphic conditions, constrained by the mineral equiblia, indicate temperatures of 560-640°C at a minimum pressure of 10 kbar. The metamorphism is dated at 64-84 Ma (Aygül et al., 2012). To the southeast, the KMC is in tectonic contact with the Çetmi Mélange (ÇM) which is an accretionary ophiolitic mélange consisting of limestone, basalt, serpentinite, greywacke, radiolarian chert and metabasite.

The KMC and ÇM are intruded by the Gürece Pluton, U-Pb LA-ICP-MS dating of which yielded Mid-Eocene age (46.19±0.74 Ma; Korkmaz et al, 2012). From several granitoid intrusions of similar ages along the southern coast of the Marmara Sea (Fig. 1B), the Gürece Pluton consists of coarse-grained equigranular granodiorite and quartz monzodiorite, cut by occasional aplitic veins. Both the KMC and ÇM are unconformably covered by Late Eocene volcano-sedimentary successions.

2.1 Gürece Pluton

On the 1:100.000 scaled geological map of the region, Duru et al. (2012; Fig. 2) show the Gürece pluton and the country rocks as series of Kemer mica schists but they haven't marked the roof pendant consisting the Bakırlık Tepe contact aureole in their map and the ÇM rocks to the northwest of the pluton. The Gürece Pluton is exposed in the northern part of the Biga Peninsula between the towns of Biga and Lapseki. The pluton shows a deformed diamond shape (Fig. 2) and covers an

area of 25 km^2. The main facies of the intrusive rocks is hornblende quartz monzonite, a very homogeneous relatively coarse-grained body (grain size 1 to 4 mm). Quartz, plagioclase, K-feldspar and hornblende are visible to the naked eye. The sparse biotite is mainly present in the marginal facies. The presence of centimetric euhedral phenocrysts of orthoclase is almost universal. Typical unaltered samples are observed in deep valleys of Biyet Dere, Derin Dere and Değirmen Dere around the Gürece village (Fig. 2). The mafic enclaves are very rare. Petrographic study of monzonite (G-4 location on Fig. 3, Fig. 4 A, B) shows a mineralogical association of orthoclase (27-35 vol. % of all) sometimes as megacrysts which give the rock a porphyric appearance, oligoclase-andesine (29-39 vol. %), anhedral quartz (12-16 vol. %), euhedral green hornblende (20-25 vol. %) and large crystals of dark brown biotite (5-10vol. %) and euhedral magnetite (1-2 vol. %).

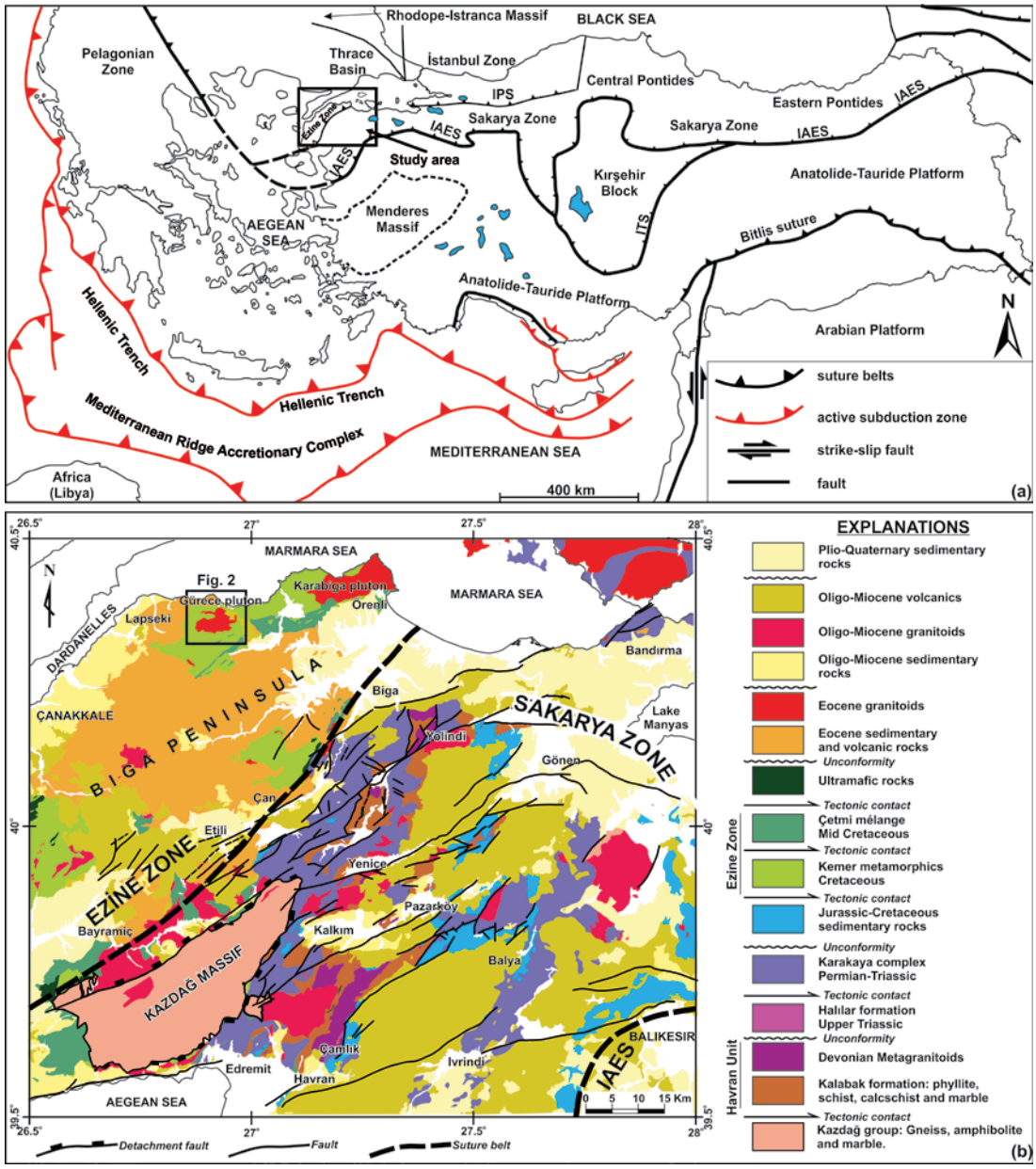

Figure 1. Geological map of NW Turkey: (a). Tectonic map of Turkey with major suture zones (Okay and Tüysüz, 1999; http://giseurope.brgm.fr/Tethyan/WTethysideMed2.gif). IPS: Intra Pontide suture, IAES: Izmir-Ankara-Erzincan suture, ITS: Inner Tauride suture. (b) Simplified geological map of the Biga Peninsula and surroundings area (after Duru et al., 2012).

In the study area two different intrusive bodies show sharp contacts with monzonite:

- On the West, there is a mass of monzodiorite (Md in Fig. 2), formed probably due to transformation of magmatic rocks in contact with the mafic country rocks.

- On the East, there is alkali feldspar granite (Agr in Fig. 2) which is well-exposed in the Değirmen Dere valley. This granite, displaying microgranular texture, is often altered and is composed of alkali feldspar (45 vol. %), albite and altered plagioclase (21 vol. %), quartz (33 vol. %) and biotite in small quantities (Öngen, 1992).

Gürece pluton cuts the KMC and rocks of multiple origins from the ÇM. SiO_2 contents and ASI (Aluminum Saturation Index) values of the intrusive rocks vary between 56.05-65.63 % and 0.87-1.04, respectively. The Gürece pluton is therefore classified as a metaluminous - peraluminous, I- type granitoid. K_2O contents show that the pluton is a high-K calc-alkaline granitoid. Variation diagrams give evidence that fractional crystallization played an important role during its formation. Upward concave patterns on the chondrite-normalized REE spidergrams are indicative of high degree of plagioclase and amphibole fractionation. Plotting on discrimination diagrams, all granitoid samples fall into the volcanic arc granitoids (VAG) field (Korkmaz et al, 2012).

2.2 Contact aureole of Bakırlık Tepe

At NE of Gürece village, near Bakırlık Tepe hill (154 meters altitude) the greywacke and a pile of limestone, probably an olistostrome in the Çetmi Mélange crop out in a roof pendant (0.7 km^2; Fig. 3).

Limestones from the ÇM crop out as olistostromes near Örenli village (Fig. 1) south of Karabiga pluton contact. These blocks has a nearly calcitic core and is surrounded by impure carbonate crust (Keskin, 2002). A similar elongated block of marble crop out in the Bakırlık Tepe contact aureole, which suffered intense skarn alteration (Fig. 3). At Bakırlık Tepe hill, these rocks are partially enclosed by the intrusion. The two cross sections show the superposition of rock types in the aureole (Fig. 3). Further east, connected to the body of marble (Fig. 5), a small area of contact is well-exposed between the marble and pyroxene skarn (Fig. 3; location 5). This clear hornfels is fine-grained and very hard to break, originated from limestone crust of olistoliths.

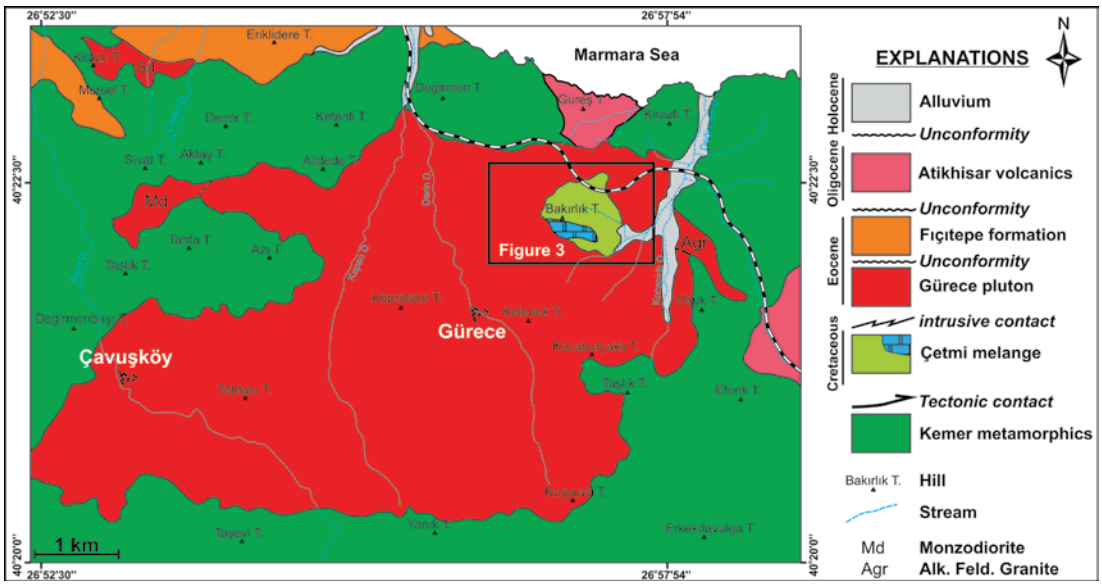

Figure 2. Geological map around Gürece pluton (Çalapkulu, 1976; Duru et al., 2012), Frame: Roof pendant at Bakırlık Tepe (detail in Figure 3).

The mineral distribution in the hornfels is homogeneous, lacking layering and bears composition of impure limestone parent like the marble crusts to the north of Örenli village, near Karabiga (Fig. 3; marble crust). They have a variable appearance, ranging from almost entirely of calcium silicates minerals

to silicate marbles (50 % calcite at most; Fig. 6A; Fig. 8, Fig. 9D). The silicate mineral constituents are grossularite (Ad_{17-20}, a = 11.873 A°), wollastonite and few diopside (due to its 1.81% MgO in hornfels chemistry). Plagioclase is absent. Quartz is detected by X-rays and the apatite is observed optically. Calcite contains no Mg or Mn. Small prisms of wollastonite, distributed regularly in the rock are idioblastic; triple cleavage is characteristic in transversal sections (Fig. 6B). In general, all grains have the simple twinning of (100), along the axis (010). The value of 2V = 30-40° is a little low. The isotropic colorless grossularite is xenoblastic, showing "amoeboid" sections and tends to include other constituents, particularly wollastonite (Fig. 7D; G-26A).

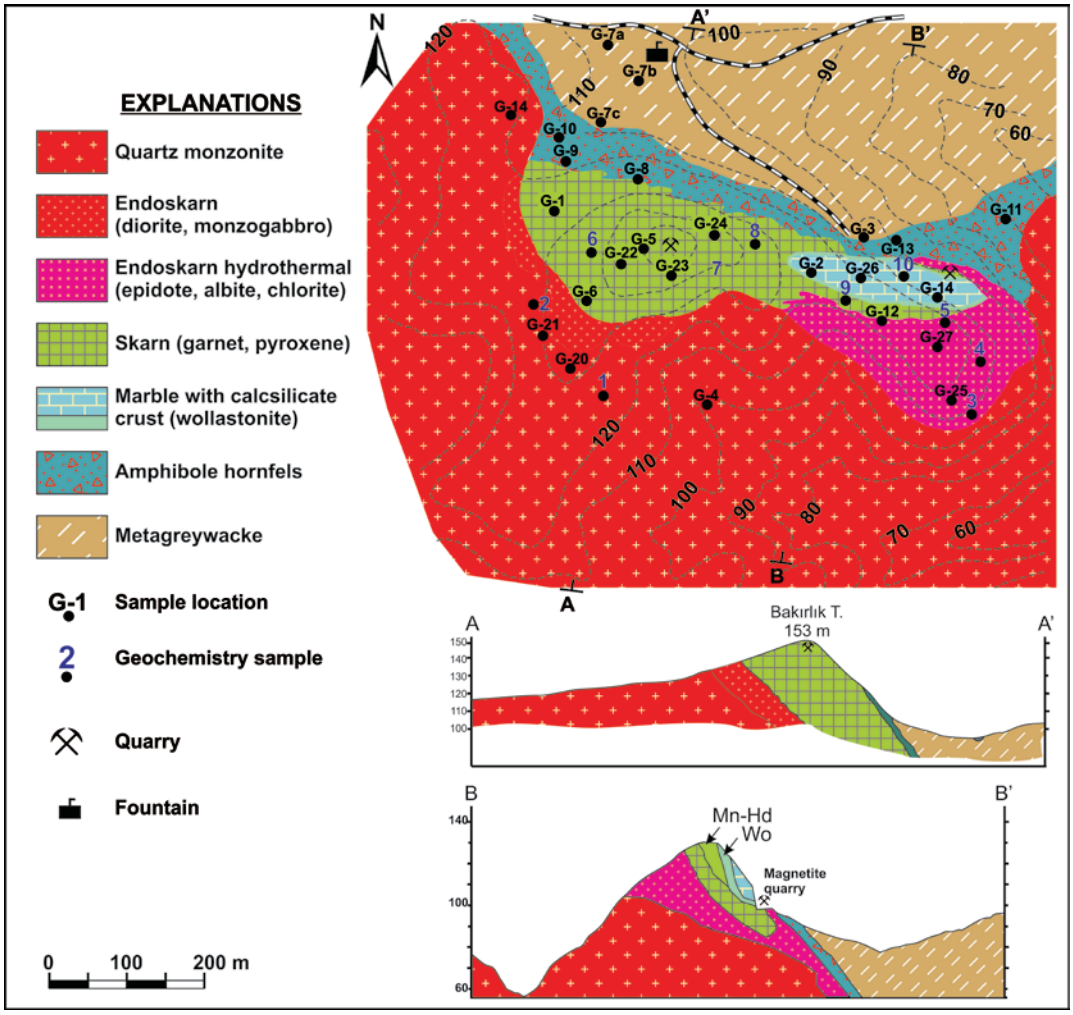

Figure 3. Geological map and cross sections of Bakırlık Tepe, NE of Gürece village.

Pure calcitic limestone, recrystallized during the contact metamorphism, is transformed into a coarse grained marble with large crystals of calcite (Fig. 5). In outcrop, these rocks are blue-grey in weathered and white in fresh surfaces. Stratification or layering is absent. Under the microscope, the polygonal mosaic texture contains coarse (3 cm) equigranular calcites and rounded fine crystals of diopside, located at triple points (Fig. 6C). All calcite crystals show undeformed polysynthetic twins. The mineralogical assemblage of green-brownish hornblende + anortite reflects typical granular hornfels texture, later cut by skarnoid assemblage of Fe-salite+garnet (Fig. 6D).

In the contact aureole greywackes from ÇM (Fig. 6E and 6F) are transformed into cordierite bearing pelitic hornfelses (Fig. 7A).

3. ANALYTICAL TECHNIQUES

Mineral chemistry analyses were performed using a Cameca SX50 electron microprobe (5 wavelength-dispersive spectrometers) at Service Laboratory of University of Nancy - I (France) by the first author. Analyses were carried out using an accelerating voltage of 15kV, a beam current of 20 nA, counting interval 13sec and a beam size 1 μm. Major oxides and trace elements were analyzed at CNRS-CRPG laboratories in Nancy (France) by XRF and wet chemical analyses.

4. PETROGRAPHIC DESCRIPTION OF BAKIRLIK TEPE SKARN

Bakırlık Tepe aureole covers an area of 600 x 200 meters surrounded by monzonite of Gürece pluton. In this roof pendant of ÇM, the rocks have been subjected to a high degree of contact metamorphism: greywacke, siltstone and clayey limestone were transformed to meta-greywacke, quartzite, hornblende-hornfels and marble, respectively (Fig. 3). Typical polygonal hornfels texture with triple points is well-formed in all these rocks. Nearly 2/3 of marble volume was altered to calcic skarn. The endoskarn and exoskarn zones are well-developed (Fig. 8).

Skarns are distinguished according to their spatial position:

* Endoskarn is formed by replacement of granitoid rock.

* Exoskarn is formed by replacement of impure carbonate rocks.

The boundary between the two types is often not clear in the field but the exoskarn zone covers larger area and bears disseminated metallic minerals.

4.1. Endoskarn

The endoskarn has two zones of variable thickness, ranging from 0 to 40 meters. The mineralogical and chemical compositions of these "endoskarns" are shown in Table 1. The endoskarn textures vary from hypidiomorphic-granular to ophitic. The two types of endoskarns, one dark and one light in color, can be distinguished based on their mineralogical compositions (Table 1; Fig. 8):

Dark endoskarn at garnet skarn contact (monzodioritic; Fig. 4B): Its outcrops are at immediate contact to exoskarns. The existence of obvious magmatic character is marked by a relict granular, highly fractured texture and especially by the presence of K-feldspar similar to those in the monzodiorite (Fig. 4B). The plagioclases are partially replaced by hydrated minerals such as sericite, epidote and prehnite. Magmatic hornblende is absent in this zone. Few grossularite and sphene are disseminated in the rock. Aluminous garnet presents crystal segregations from originally anhedral grains (Fig. 7B). The isotropic core of the crystal is very homogeneous and brown in color while the anisotropic rims contain abundant fluid inclusions.

Table 1: Zonation of skarns in Bakırlık Tepe contact aureole.

<table>
<tr><td rowspan="3">Quartz Monzonite</td><td rowspan="3">Diorite</td><td>Dark Endoskarn (G-20)</td><td colspan="3">Clear Endoskarn (G-21)</td><td>Ore</td><td>Prograde Skarn</td><td rowspan="3">Marble</td></tr>
<tr><td>Monzodiorite
Magmatic texture
Pl+Qu+Hb±Bi+Sph+Zr
Pl An_{59-36} Unzoned
Hb with relict cpx
Act-Hbc+Act-Mg Hb
Chl pennin (Bi)
Magnetite</td><td>Amphibole monzonite
Granular texture
Pl Lab-And
Core Trem, Rim Mg Hb
Sph
Ap</td><td>Diopside monzonite
Granular texture
Pl Lab-And
Pale green cpx Hd_{27-23}
Sph (abundant and cores)</td><td>Garnet endoskarn (G-6)
Relict magmatic texture
Altered Pl
Grossularite
Sph
Qu</td><td>Fe</td><td>Garnet skarn
Inner zone
near granitoid
(Fig. 3; No: 6 and 7)
Outher zone
covering marble
(Fig. 3; No: 9)</td></tr>
<tr><td colspan="2">Monzogabbro (G-27)
Granular texture
Pl Byt+An
Green cpx Hd_{24}
Bi Ep+Chl altered
Ap abundant
Sph
Chalcopyrite</td><td colspan="2">Transition Zone
Granular texture
Cpx Hd_{24-35}
Inverse zoning An_{67}- An_{85}</td><td>Passage to calcic skarn
Granoblastic texture
Cpx Hd_{40}
Or_{90}
Pl Lab</td><td>Zn</td><td>Pyroxene skarn
Inner zone dominated
by garnet
Main skarn zone
dominated by
Mn-cpx</td></tr>
<tr><td colspan="9"><.....Endoskarn 0-40 m.....> <.....Exoskarn 150 m.....></td></tr>
</table>

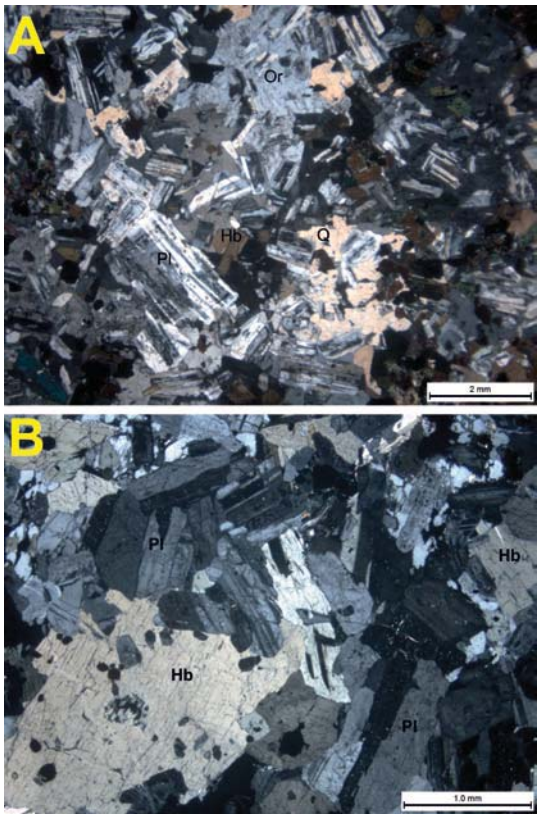

Figure 4. Petrographic microphotographs of samples. A. Main facies of Gürece quartz monzonite, SE of Bakırlık Tepe; G-4); B. Endoskarn transformation of monzonite (hornblende diorite; G-20).

4.2 "Hydrated" endoskarn (Light endoskarn)

A light endoskarn was observed at pyroxene skarn contact (monzogabbro; Fig. 7C): it is surrounded by epidote endoskarn ("hydrated" endoskarn). It seems an advanced transformation of diorite (Fig. 3; No. 5 and Table 1). The epidote-bearing endoskarn follows the quartz monzonite contact. This endoskarn is more extended, but more or less continuous along the contact and shows fine layered structure in which olive green epidote-rich layers alternate with white colored feldspar + quartz + calcite layers, that are parallel to the monzonite contact.

Irregular dark green chlorite spots can be distinguished by naked eye. Chlorites have a radial texture and show anomalous brown interference colors and negative elongation under the microscope. Microprobe analyses of chlorites show a clear zonation, where manganese enrichment is observed at the crystal rim (MnO = 2.50%; Table 2) (Fig. 7D). The chlorite beds represent probably the ferro-magnesian minerals of monzonite. The chemical analysis of the rock (Table 3) indicates higher levels of Sr and V because of epidote enrichment (advanced alteration of plagioclase).

4.3. Exoskarn

The exoskarn with garnet skarn and pyroxene skarn bands has a thickness of 150 meters. This zone consists at majority of a dark brown idioblastic garnet, which has small geodes filled either by magnetite and iron hydroxides, or calcite and quartz. Progressively towards the east of Bakırlık Tepe (Fig. 3a), this garnet skarn appears to have replaced most of the marble zone. In the marble quarry (Fig. 5, No. 10), an elongated part of the pure calcite marble survived skarn processes.

Figure 5. Marble block at Bakırlık Tepe.

4.3.1 Garnet skarn

Two different zones can be defined as the inner and the outher zone in the garnet skarn.

The inner zone, dominated by garnet skarn, is made up almost entirely of idioblastic garnet crystals. The individual garnet crystals in this massive body show two crystallization stages. In the crystal core, brown garnet is isotropic and has an average composition of Ad_{90} but near the rim, it is anisotropic and its composition varies around Ad_{70} (Fig. 9A, G-1). The negative correlation between Fe and Mn and positive correlation between Al and Mn are very obvious (Fig. 10). The envelope of the crystal grew around without replacing the first. Boundary between the core and the rim is sharp. MnO values are quite high (max = 3. 6 wt. % MnO, Table 2) along the crystal. Both garnet and pyroxene contain primary fluid inclusions (inclusions of liquid H_2O and CO_2).

Table 2: Representative analyses of Bakırlık Tepe skarn minerals. Structural formulas calculated on the basis of: pyroxenes, 6 oxygens; epidotes, 12.5 oxygens; garnets, 24 oxygens; chlorites, 28 oxygens; wollastonite, 18 oxygens.

	Pyroxenes				Epidotes			Garnets						Chlorites		Wollastonite
	G-5	G-5	G21	G-27	G-25	G-5		Gu-1	G-1	G-24	G-26a	G-26c	G-26c	G-25	G-25	G-26a
SiO_2	50.62	50.15	50.80	49.67	39.64	38.00		36.75	36.76	36.55	39.15	38.64	36.51	29.55	29.52	51.49
TiO_2				0.49	0.11					0.06	0.56	0.21	0.01	0.05		
Al_2O_3	1.06	0.06	0.09	3.16	29.54	22.17		8.82	6.96	0.39	15.53	6.30		18.59	19.49	0.05
Fe_2O_3		0.23		4.01	5.29	14.40		19.29	19.07	27.03	5.53	21.35	29.22	13.58	14.30	
FeO	9.41	10.92	8.39	9.57					1.83							0.12
MnO	12.29	11.2	0.50	0.34	0.76	1.36		3.63	2.46	0.14	0.12	0.42	0.19	2.50	2.12	0.11
MgO	4.23	4.22	12.48	10.06	0.12					0.41	0.42	0.11	0.15	22.92	22.59	0.21
CaO	22.74	23.13	25.18	23.45	23.20	21.18		31.91	29.29	33.83	36.16	34.42	33.54		0.06	0.06
Na_2O	0.03	0.04	0.12	0.41											0.04	0.06
K_2O	0.07		0.03													
ZnO	0.26	0.41														
Total	100.71	100.38	100.59	101.17	98.66	97.11		100.40	96.37	98.41	100.47	101.45	96.62	87.19	88.12	100.61
Oxygens		6			12.5					24				28		18
Si	1.994	1.996	2.006	1.874	3.034	3.059		5.954	6.197	6.205	5.961	6.172	6.156	5.924	5.861	5.952
Al^{iv}	0.006	0.004		0.126				0.046			0.039			2.076	2.139	0.007
Al^{vi}	0.043		0.004	0.015	2.665	2.103		1.638	1.383	0.078	3.286	1.186		2.316	2.422	
Ti				0.014	0.006					0.007	0.064	0.025	0.001	0.008		
Fe^{3+}		0.007		0.114	0.305	0.872		2.352	2.419	3.453	0.634	2.567	3.707			
Mg	0.248	0.250	0.694	0.566	0.014					0.103	0.095	0.026	0.037	6.848	6.685	0.037
Fe^{2+}	0.310	0.364	0.262	0.302					0.259					2.277	2.374	0.011
Mn	0.410	0.378	0.016	0.011	0.049	0.093		0.498	0.351	0.020	0.015	0.056	0.027	0.424	0.357	0.011
Ca	0.960	0.986	1.006	0.948	1.902	1.827		5.539	5.291	6.153	5.899	5.891	6.059		0.013	6.015
Na	0.003	0.003	0.009	0.031											0.015	0.013
K	0.004		0.001													
Total	3.985	4.000	3.998	4.001	7.975	7.954		16.030	15.000	16.020	15.990	15.920	19.990	19.870	19.870	12.050
							Pyr			1.64	1.58	0.43	0.60			
Mg	12.86	12.59	35.09	29.16	Ps %		Alm		4.38					XFe		
Fe+Mn	37.34	37.73	14.05	22.00			Spe	8.24	5.94	0.31	0.24	0.93	0.44			
Ca	49.79	49.67	50.86	48.84	10.3	29.3	Gross	33.34	28.21	15.37	80.77	33.56	8.15	0.25	0.26	
							And	58.42	61.47	82.67	17.41	65.07	90.81			
Mineral	Mn-Hd	Mn-Hd	Di	Fe-Di	C-Zo	Ep		Mn-And	Mn-And	And	Gross.	Gross-And	And	Mn-Chl	Mn-Chl	Wo

Table 3: Whole rock chemical analyses from granitoid rocks and skarns of Gürece contact aureole (major elements in wt. %, trace elements in ppm).

	G-20	G-21	G-25	G-27	G-26a	G-22	G-23	G-24	G-26c	G-28
SiO_2	55.65	54.24	42.75	44.03	25.42	42.34	31.83	31.51	18.96	0.08
TiO_2	0.97	0.76	1.33	1.87	0.08					
Al_2O_3	17.26	19.10	21.96	18.04	2.68	0.52	2.29	1.04	0.22	
Fe_2O_3t	6.79	4.62	8.83	9.07	1.12	5.97	9.35	28.35	32.32	
MnO	0.13	0.08	0.46	0.13	0.06	1.45	1.64	0.46	0.28	
MgO	4.01	4.19	2.61	5.12	1.81	5.37	3.16	0.97	0.14	0.44
CaO	8.51	9.98	16.26	17.31	46.96	24.14	28.33	28.87	34.53	56.82
Na_2O	4.10	4.69	1.31	1.38						
K_2O	0.81	0.32	0.17	0.29				0.05		
H_2O+	1.27	1.39	3.40	2.12						
CO_2					21.57	19.91	23.04	7.70	13.78	42.04
P_2O_5	0.26	0.41	0.30	0.36	0.06	0.28	0.20	0.17	0.22	0.06
Total	99.76	99.78	99.38	99.72	99.76	99.88	99.84	99.12	100.45	99.44
Ba	317	175	104	88	5	5	7	5	5	3
Be	1.2	1.5	1.7	0.8	0.5	2.9	3.0	0.5	0.5	0.5
Co	32	44	22	51	9	147	87	30	50	5
Cr	19	25	301	433	22	25	11	17	13	7
Cu	8	6	529	82	36	5	60	7	74	6
Ga	18	24	41	20	12	12	12	18	5	10
Nb	10	7	26	34	5	5	5	5	5	5
Ni	6	17	67	125	18	12	16	22	21	14
Rb	17	7	9	12	10	7	7	16	19	18
Sc	22.3	31.0	39.5	45.7	7.0	1.5	2.2	2.6	2.7	2.2
Sr	387	459	1735	489	1188	144	190	60	53	335
Th	5	5	26	6	16	7	8	5	5	20
V	177	191	186	251	17	36	111	38	13	5
Y	29	40	41	35	21	5	5	5	5	5
Zn	53	42	958	85	44	376	208	14	26	8
Zr	141	314	311	113	24	5	10	18	21	5
Sample Position (Fig.3)	1	2	3	4	5	6	7	8	9	10

Only the garnets of sample G-1 contain large isolated inclusions (up to 300 microns). The majority of the primary fluid inclusions are found in the growth zones.

Secondary fluid inclusions are observed only in the interstitial quartz. Garnets in contact with pyroxene skarn (G -24) show idioblastic faces at the end of their growth zone and interspaces are filled by mainly Mn-bearing calcite (MnO = 1.6 %). All crystal cores contain rosettes of hematite (Fig: 4b).

The outer zone, surrounding the marble starts with a massive skarn which is granular, yellowish-brown colored at outcrop (Fig. 3; location 9). The secondary minerals are red hematite and clear white calcite. Under the microscope, individual garnet crystals are uniformly brown colored and isotropic; microprobe analyses show a weak zonation: Ad_{83} in the core and Ad_{96} at the rim (Huckenholz et al., 1971). Unlike the inner skarn area, Mn or fluid inclusions are absent (Fig. 9C; G-26c). The massive skarn with a thickness of about 3 meters surrounds the marble zone and is observed in the field along the contact with the marble through 60 meters. The idioblastic megacrystals of garnet show perfect growth zoning. In quarry, many centimeters long isolated crystals can be found in the calcite matrix. All crystals contain magnetite in core (Fig. 9B).

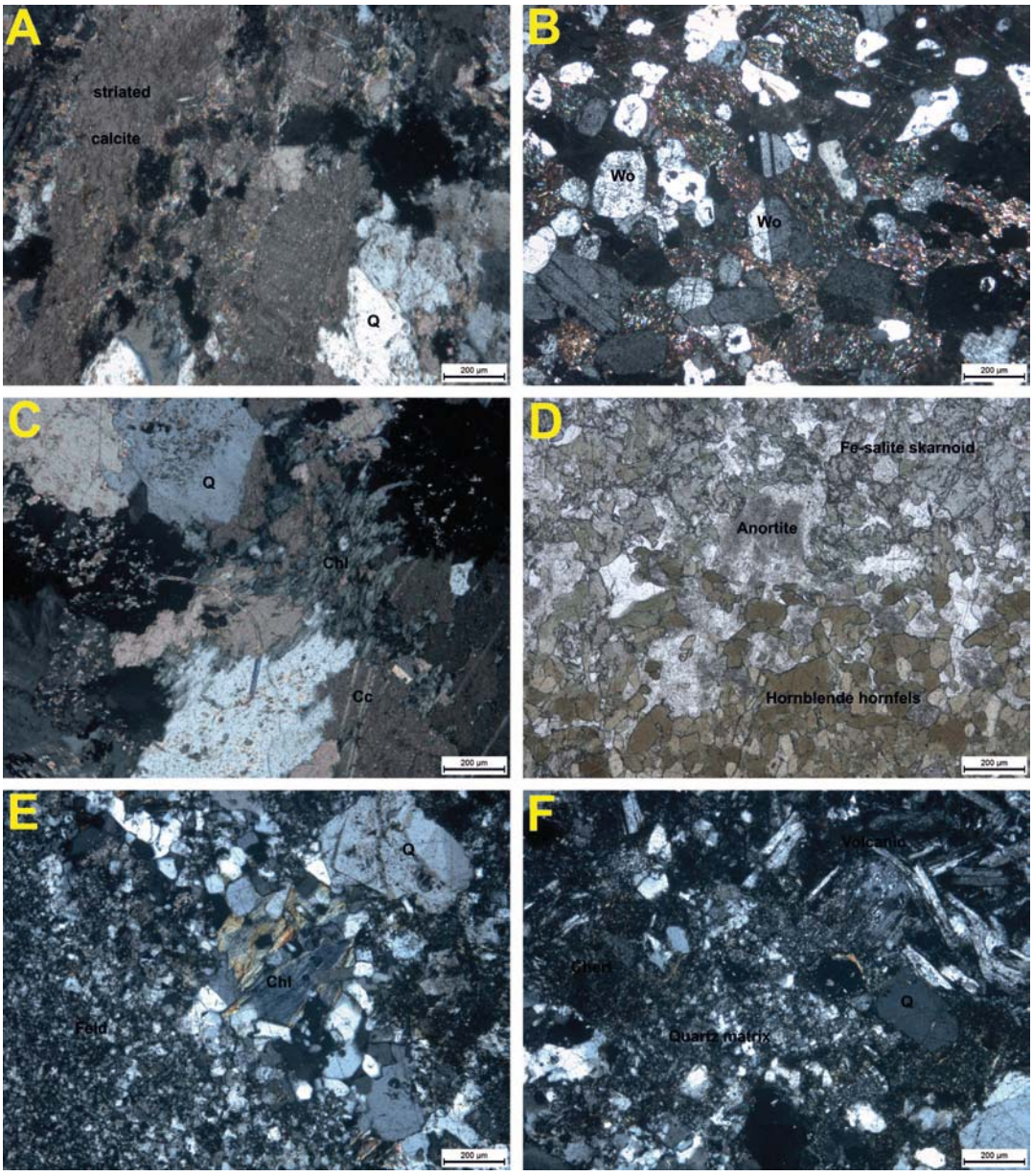

Figure 6. Petrographic microphotographs of samples. A. Calc-silicate hornfels, note wollastonite ghosts on calcite crystals (G-22); B. Calc-silicate hornfels bearing wollastonite (in marble crust; G-26c); C. Calc-silicate hornfels with chlorite (impure limestone; G-23); D. Pyroxene (Fe-salite+plagioclase) skarn infiltrates contact metamorphic amphibole hornfels which is an alteration of impure marble (G-9); E. Metagraywacke with chlorite from Çetmi Mélange (G-7a); F. Metagraywacke with volcanic rock particles (G-7b); G. Metapelitic hornfels bearing cordierite and K-feldspar (G-7c).

4.2.2 Pyroxene skarn

The pyroxene skarns form irregular and elongated bodies or spots in garnet skarn at Bakırlık Tepe. There are also yellow garnets dispersed within blue-green pyroxenes (Fig 3, dot symbols between No. 6 and No. 7). The arrangement of these minerals reveals the replacement of pyroxene by later garnets. There are two different zones:

The inner zone dominated by garnet: garnet-bearing granoblastic texture makes 70 % of the volume of this zone (Fig. 3 cross sections). They are less anisotropic and show sector twins (Fig. 9a).

The composition is generally intermediate in the grossularite-andradite series (Ad_{58}), but in contact with the pyroxene zone, Fe and Mn are enriched (Ad_{68}; MnO = 1.4 wt. %). The pyroxenes show the same tendencies (i.e. Fe-diopside is enriched in Mn). Some interspaces are filled by epidote (Ps_{26-29}).

The main area dominated by pyroxene: this zone is occupied by a particular pyroxene; an idioblastic, medium-grained hedenbergite. The optical characters include: high relief, rose color, yellow first order interference color, biaxial positive, 2V=80º, Z^c = 45 (value greater than diopside), the elongation l = (+), normal extinction in the (010) zone. Near the garnet zone, the pyroxenes show polysynthetic twins similar to that of plagioclase (Fig. 7E; Table 2: G-5).

At crystal rim the pyroxene is represented by a composition close to the ferro-johannsenite but the 50 % mol limit of $CaMnSiO_3$ was not crossed. In general, these metasomatic pyroxenes are Mn-hedenbergites. Analyses of pyroxene are plotted (Table 2, G-5) on a triangular diagram of Jo-Di-Hd (Fig. 11a, b): two populations can be distinguished substituting an alternative range of Fe-Mn^{2+}, which maintains constant values of Mg and follows an evolutionary trend toward johansenite corner. It seems that towards the garnet zone these pyroxenes have twins and show the highest Mn enrichment (Fig. 7E).

5. GEOCHEMICAL STUDY OF THE AUREOLE

One of our research focuses on the interpretation of metasomatic zoning caused by geochemical transfer (variation of mobile elements; Table 3). In metasomatic exchange between two contrasting lithologies, the chemical analyses allow identification of the original limit of the pluton and thus the distinction between endoskarn and exoskarn can be made.

The major elements:

- Silica steadily decreases from granitoid to marble while calcium increases gradually toward the intrusive rock. There are two steps:

First step: Progressive appearance of pyroxene in endoskarn at the expense of biotite and hornblende and disappearance of calcic plagioclase (endoskarn contains 15% CaO, while CaO is only 3% in the parent intrusive rock).

Second step: Significant development of garnet and/or pyroxene (then CaO exceeds 25%). The high value of calcium in wollastonite hornfels reflects strong presence of calcite in the carbonate host rock.

- Al values show high contrast between the granitoid and skarns. The peak value of Al is encountered in the endoskarn.

- The garnet skarn and retrograde pyroxene skarn can be separated according to the distribution of Mg.

- Enrichment of total Fe in the garnet skarn indicates magnetite mineralization in the samples.

- Mn concentration is in good correlation with rocks that contain manganeferous minerals such as Mn-chlorite. Altered pyroxene skarn and "hydrated" endoskarn are both rich in Mn-chlorite.

The trace elements (Be, Cr, Cu, Nb, Ni, Sc, Sr, Th, V, Y, Zn, Zr; Table 3): in general, show enrichment only in the endoskarn. A few features are apparent: Ba gets depleted rapidly in the granitoid and is absent in the skarn. Sr profile shows a double peak due to epidote enrichment in the hydrated endoskarn and in the calc-silicate hornfels. Zn is very significant in hydrated epidote endoskarn and in pyroxene exoskarn (zinc-bearing pyroxene). Hydrated pyroxene skarn is enriched in Be.

6. DISCUSSION

6.1. Prograde skarn

In calc-silicate hornfels, the composition of garnet highlights the initial conditions of a relatively high activity of CO_2, as might be expected in carbonate sediment parents. The homogeneity of grossularite composition shows that the participation rate of CO_2/Fe^{3+} was more or less regular during the early stages of metamorphism. The rock has undergone a rapid heating. At this stage, the activity of CO_2 has been considerably increased due to the decarbonation of limestone, and grossularite was the stable phase. This confirms also the early crystallization of wollastonite and indicates a downward trend in temperature while XCO_2 decreases (Taylor and Liou, 1978) at temperatures above 600°C and a maximum XCO_2 of 0.15. Following the crystallization of grossularite, it reaches a minimum temperature of 500°C at 2 kbar (450°C and 1 kbar) and the fluid phase is enriched in H_2O (Meinert, 1992; Meinert et al. 2005).

In endoskarn, contamination has a large radius of action. The boundary between the diorite and endoskarn is very sharp and the disappearance of hornblende and biotite in favor of pyroxene gives a clear rock without significant change in magmatic texture. On the other side the development of retrograde endoskarn ("hydrated") in contact with the

limestone is the result of the following reaction:

Calcic plagioclase + calcite + H_2O ---> clinozoisite + albite + CO_2 (1)

The presence of epidote is very dependent on the partial pressure of CO_2 (CASH system). According to the (CO_2 /T°C; Bucher and Grapes, 2011) equilibrium curve of the reaction (1), in the absence of quartz, we deduce that clinozoisite was stable at very different temperatures and very low partial pressures of CO_2 (XCO_2 less than 0.03). The "hydrated" endoskarn enriched in epidote is an extreme example of the transformations at low temperatures. It comes as a result of metasomatic reactions in the interspace between the monzonite and the marble, with a fluid that is released during the pneumatolytic phase and remains trapped in the limestone wall, acting as a barrier.

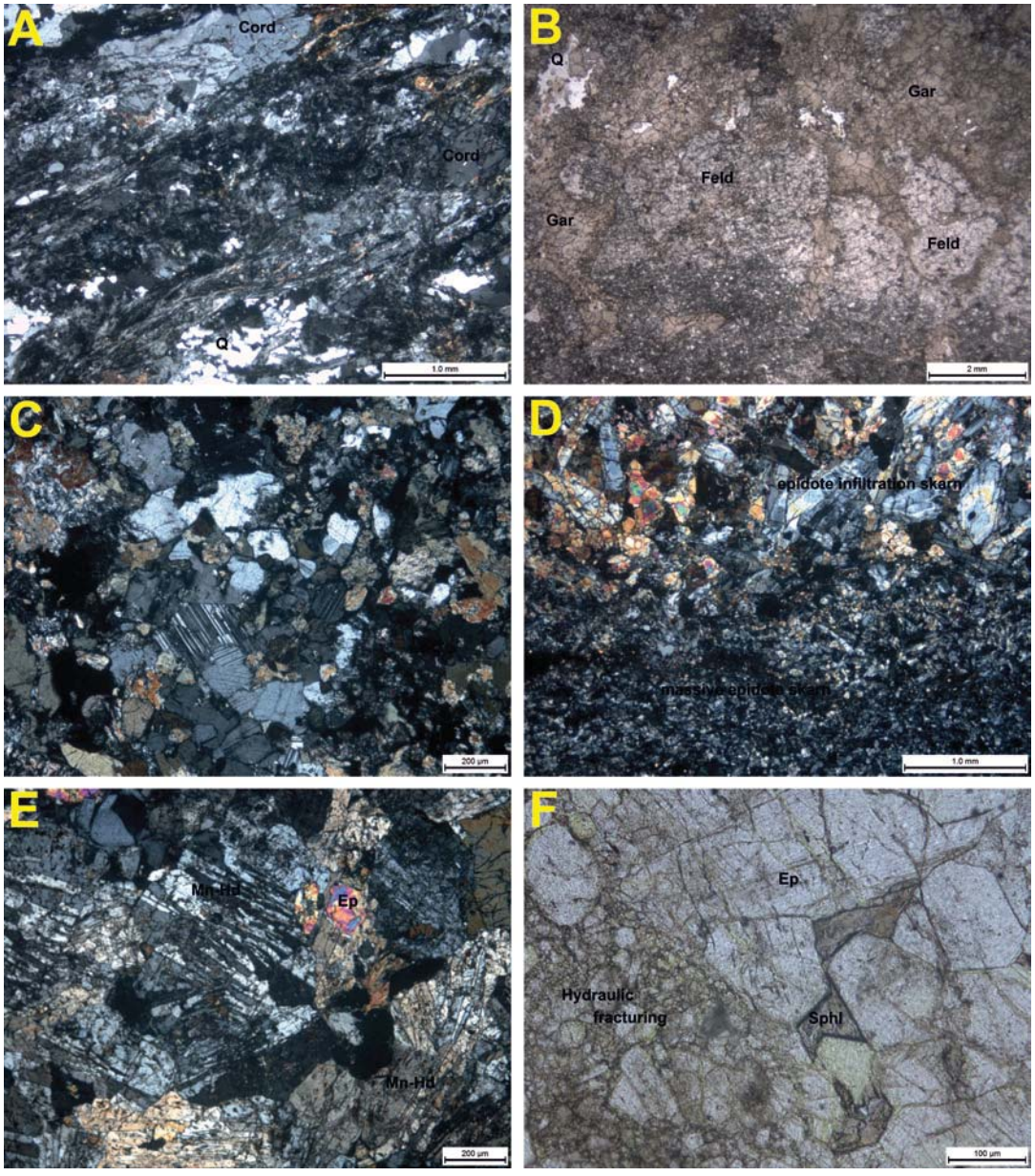

Figure 7. A. Metapelitic hornfels bearing cordierite and K-feldspar (G-7c) B. Garnet endoskarn: advanced transformation of monzonite (G-6); C. Endoskarn transformation "monzogabbro" (G-11); D. "Hydrated" epidote skarn infiltrates contact metamorphic amphibole hornfels (G-25); E. Mn-pyroxene skarn (johannsenite) and epidote (G-5); F. Hydraulic fracture zone in pyroxene skarn bearing sphalerite (Fig. 7F, location G-5). Abbreviations: Gar: Garnet, Feld, Feldspar; Ep: Epidote, Mn-Hd: Mn-Hedenbergite, Cc: Calcite, Sphl: Sphalerite, Q: Quartz, Pl: Plagioclase, Or: Orthoclase, Hb: Hornblende, Chl: Chlorite, Cord: Cordierite, Wo: Wollastonite.

In other words, the impermeable mass of marble probably prevented the free movement of fluids and accumulated in an enclosed space in the endoskarn area that promoted the formation of the mineral phases at low temperature (Fig. 12).

Iron mineralization is only observed in the garnet exoskarn but the marble and calc-silicate hornfels do not contain iron. Whole rock chemical analyses of skarns plot in the field of calcic skarn. Ca-Mg-Fe diagram (Fig. 13) may well-explain the low iron-bearing ore development in the aureole and the distribution of Fe between calcic hornfels through pyroxene skarns to andradite corner. The main skarn shows discordant development facing to the elongated axis of the host rock as can be seen in the field (Fig. 3). The western part suffered intense metasomatism, while some parts of the marble remain unchained in the east, where marble is farthest from the magmatic contact.

Endoskarn	Transition zone	Calcic Pyroxene Skarn
Granular texture	Xenomorphic grains	Granoblastic texture with poikiloblastic plagioclase
Or_{80} Biotite (chlorite) Apatite Cpx Hd_{20} Plag An_{70-80} Sphene (coarse) Chalcopyrite	Cpx Hd_{30} An_{80}	Or_{90} Cpx Hd_{40} An_{65-70} Sphene (small) Bornite

Figure 8. Endoskarn of monzogabro composition in contact with pyroxene skarn (G-27 sample from epidote skarn to the east of Bakırlık Tepe). Monzogabbro has a thickness of some tens of centimeters.

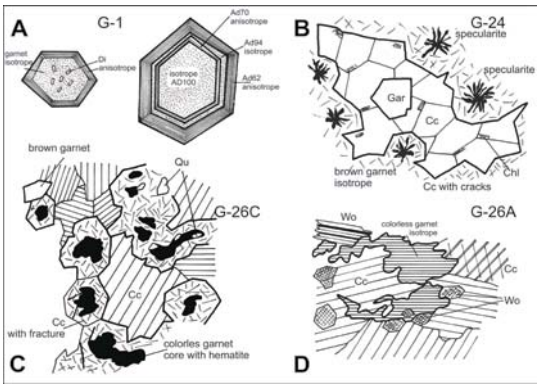

Figure 9. Garnet habitus at contact: A. Adjacent the prograde skarn/granitoid contact (G-1): Idioblastic crystal showing two stages of crystallization. Brown andradite occupies the core of isotropic crystals associated with miniscule diopside inclusions. The crystal rim is represented by a yellowish garnet, anisotropic, of an intermediate composition. The contact is sharp. Mn enrichment was detected by microprobe. B. Garnet skarn in contact with pyroxene skarn (G-24): This is a massive andradite garnet, isotropic and homogeneous in composition. Note the texture of a star shaped opaque mineral (rich in Mn and Zn) at garnet core which also contains high Mn concentration; idioblastic crystal rim is associated with the inclusion free Mn-calcite. C. Prograde skarn in contact with marble (G-26c): coarse sized idioblastic garnets (about 1 cm) are isotropic, but some chemical zoning was detected by microprobe. The cores of the crystals contain rounded quartz and hematite inclusions. D. Calc-silicate hornfels (G-26a): belonging to the stage of isochemical metamorphism these xenoblastic, isotropic and non-zoned grossularite crystals show an intergrown texture with calcite and wollastonite.

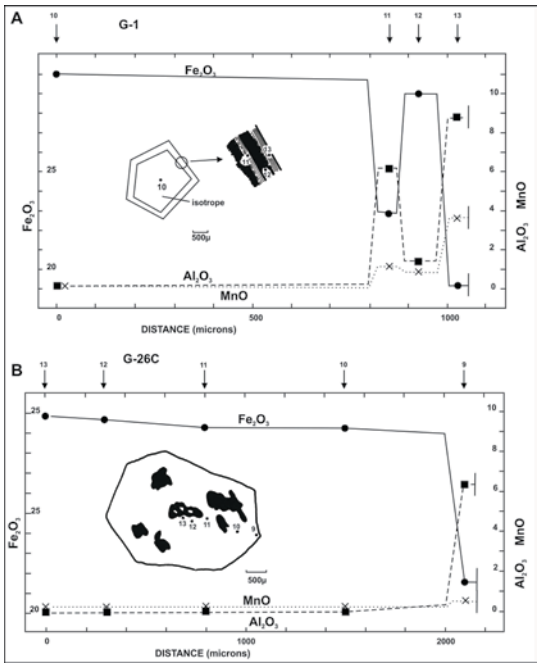

Figure 10. Representative profiles of garnet zonation: A. Garnet (G-1) derived from the inner contact area showing the isotropic crystal enclosed by an envelope zone with alternating anisotropic/isotropic character. At rim MnO content is significant. B. Garnet (G-26c) from the outer contact, bearing magnetite in the core is isotropic and at rim its composition shows variation.

The contact metamorphic transformation cannot therefore be derived from the siliceous or more iron-rich levels in the host rocks which are known to have existed in the Çetmi Mélange. We can conclude that these rocks were formed as a result of a contribution of Si and Fe. Infiltration is located inside the bay-shaped area, where a width of 150 meters can be traced. The wide spread of this phenomenon does not mean that there has been no diffusion between the igneous rock and surrounding carbonate host rock.

Diffusion phenomena induced by chemical potential gradients between two different rocks is less important. The infiltration was therefore induced by a circulating fluid between the carbonate host rocks and along the diorite/skarn contact. While two-thirds of the marble underwent total skarn alteration, beyond the marble in amphibole hornfels area, the fluid circulated only in veins or along bedding planes. The origin of these rocks is percolation metasomatism (skarnoid).

In general, the oxygen isotopic and fluid inclusion data from other similar occurrences indicate that the XCO_2 partial pressure of fluids circulating in carbonate rocks is generally low, perhaps less than 0.1 (Taylor and O'Neil, 1977).

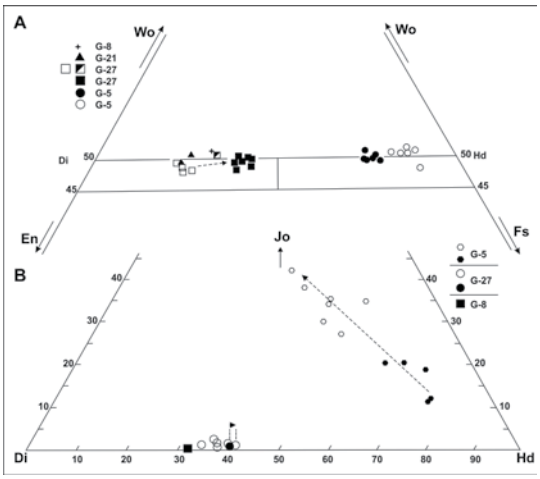

Figure 11. Ternary plots of Mn-Mg-Fe for the pyroxenes in the skarn (johannsenite-diopside-hedenbergite, mol. %; Morimoto et al, 1988). Filled symbols: crystal core; empty symbols: crystal rim.

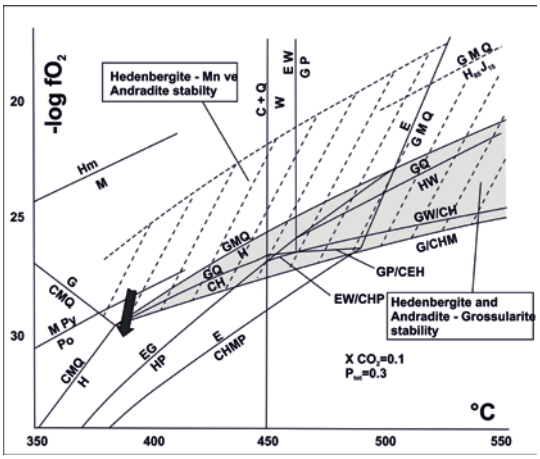

Figure 12. T - log fO_2 diagram of CaO-FeO-Fe_2O_3-Al_2O_3-SiO_2-H_2O-CO_2 system in terms XCO_2=0.1 and Ptot=0.3 kbar.

C: calcite, E: epidote, G: garnet, H: hedenbergite, Hm: hematite, M: magnetite, P: plagioclase, Po: phyrrotite, Py: pyrit, Q: quartz, W: wollastonite.

Andradite is stable below 475°C and wollastonite below 500°C. A drop in XCO_2 to about 0.01 accompanies this temperature drop of about 50° to 100°C. If it is an epizonal depth (1 kbar) a decrease of 50°C can be assumed. The crystallization

of clinozoisite + grossularite + quartz in the grain interstices indicates a minimum temperature of 400°C (if fluid phase is H_2O).

Significant alteration of pyroxene skarn: in andradite skarn replacement of magnetite by hematite (sphecularite) suggest that during the retrograde alteration the oxygen fugacity (fO_2) concentrates proximity of hematite/magnetite buffer.

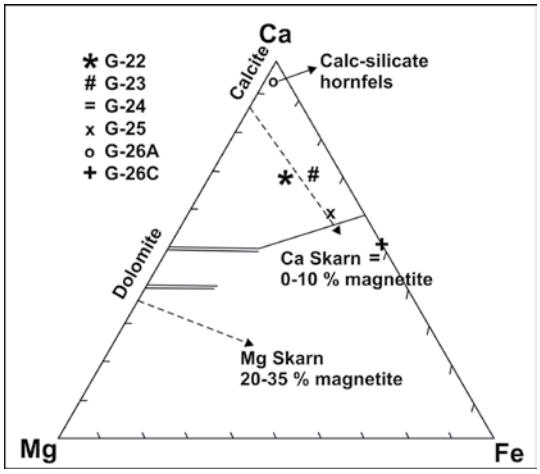

Figure 13. Ca-Mg-Fe diagram (mol. %; with SiO_2, H_2O, CO_2 and O_2) which shows the most common minerals in skarns and compatibility of phases with skarn ore deposits (Einaudi, 1982). Note that all Gürece skarn samples plot on calcic skarn evolution trend. Fe and Mg (arrows) values in skarn analyses: limestone bearing calcium skarn forms only 0-10% magnetite, while dolomite bearing magnesium skarn contains 20-35% magnetite.

After experimental studies (Gustafson, 1974), from the coexistence of andradite, magnetite and quartz in garnet cores, the following reaction could be accepted (equilibrium reaction only for silica).

$CaFeSi_2O_6 + O_2 \Rightarrow ½\ CaFe_2O_3 + SiO_2 + ½\ Fe_3O_4$ (2)

Hedenbergite Andradite Quartz Magnetite

The reaction (2), which produces andradite took place in the form of continuous reaction with decreasing fO_2. In the garnet skarn, andradite was probably formed at the expense of hedenbergitic component of pyroxene by increasing fO_2. The variations of fO_2 over a large area indicate that they were controlled from outside and not buffered internally (Gulbrandsen and Gielow, 1960).

6.2. Fluid-mineral relationships

The Bakırlık Tepe skarn system depends essentially to elongated and impermeable limestone blocks of Çetmi Mélange, which is cut and partially assimilated by the Gürece quartz monzonite. Different metasomatism phenomena are observed on both sides of the marble horizon and its carbonate crust. The elongated shape of the carbonate rocks reacted as a barrier for circulating fluids in underlying beds. As a result, two zones can be distinguished:

- The area between the marble and monzonite was dominated by a fluid rich in H_2O expelled from intrusive rocks and meteoric fluids,

- The area between the marble and metagreywacke was dominated by a CO_2-rich fluid originated from impure carbonate horizons.

The presence of clinozoisite and grossularite in the carbonate crust indicates that the partial pressure of CO_2 remained low as contact metamorphism advanced. The weak presence of wollastonite (conversely observed in Karaköy area, Öngen 1992) in contact of the marble with the garnet skarn may explain the rather low temperatures to maintain the wollastonite stability or high levels of XCO_2 in the fluid (Vidale, 1969). Metasomatic activity has created pseudomorphs from some contact originated minerals in "hydrated" endoskarn. The nature of these neoblasts (albite, Mn-Al- chlorite, clinozoisite, Mn-epidote, prehnite) indicates alkaline-silica-alumina metasomatism rich in Mn. This metasomatism, which also affected the magmatic rocks, is attributed to the action of residual magmatic fluids. The intensity of this phenomenon is explained by the presence of the marble barrier and also fluids circulating in the opposite direction in an enclosed space (i.e towards the magmatic contact) to form "hydrated" endoskarn at the expense of monzonite.

6.3. Origin of manganese

Manganiferous minerals, including pyroxene, garnet, amphibole, chlorite, calcite, sphalerite and opaque (Table 2) were identified through an E-W horizon in the skarn (Fig. 3; No.6-7-3). The manganese concentration is more pronounced in the pyroxene skarn, which occurs along the former carbonate rock contact. This skarn was developed parallel to the elongated axis of marble. According to experimental studies (Burt, 1977; Gustafson, 1974; Gamble, 1982) the following conclusions are reached for the Gürece skarn:

- The fluids forming the pyroxene depleted first Mg and Fe, and then finally Mn. This explains the presence of manganese minerals at a certain distance from the magmatic contact ("distal skarn"),

- The Mn contribution in skarns has the effect of broadening the field of stability of pyroxene (Burton et al, 1982; Fig. 12),

- Mn-enrichment of pyroxene depends on certain factors including temperature, oxidation state of the skarn, composition of the fluid phase and the water/rock ratio.

At 300°C, an addition of 15 mol. % johannsenite component in pure hedenbergite expands pyroxene stability approximately to 1.5 fS_2. This accompanies the precipitation of pyrite and sphalerite instead of pyrrhotite (Fig. 7F; G-5). Instead, for fS_2 determined, the Hd_{85} Jo_{15} is more stable below 50°C than the Hd_{100} component stability (Fig. 12; Burton et al, 1982). Yun and Einaudi (1982) suggest that low values of Fe/Mn ratio far from the contact may reflect precipitation of Fe from fluid during crystallization of andradite near the magmatic contact. In addition, Boctor (1985) determined that Mn/Fe ratio and pH have positive evolution in the system $MnO-SiO_2-HCl-H_2O$. This result is consistent with a fluid flowing through the weak zones in carbonate rock. Generally, Mn enrichment occupies on the periphery of skarn crystals (Fig. 9A, B: G-24). This phenomenon, concentrated in some places does not seem to have in common origin with marble composition, but may be explained in relation to the high content of MnO (up to 12 % MnO) in some minerals. Garnets are also Mn-rich (G-1; 4 % MnO, Fig. 9A, Fig. 10B) on top of Bakırlık Tepe than those to the east (i.e. magnetite bearing garnet skarn G-26c; Fig. 10B). This also indicates the enrichment of Mn in good correlation with the direction of fluid flow.

6.4 Zoning of metallic minerals

The zinc mineralization on Bakırlık Tepe follows the lithological contacts in the pyroxene skarn (Fig. 3; Fig. 7E). Saline fluid inclusions in pyroxene are numerous in the pyroxene skarn (study in progress). Pyroxene is Mn-hedenbergite ($Di_5Hd_{44}Wo_{51}$, 12 % MnO), enriched in Fe^{2+}, Mn and Zn. Garnet (G-5) is also enriched in Mn (Ad_{68}, 14 to 4.0 % MnO). Moreover, there is an opaque mineral containing Mn and Zn (sphalerite) in the geodes. On east of Bakırlık Tepe, the "hydrated" endoskarn shows a clear Zn-affinity resulting in manganiferous minerals and in whole rock chemistry (Table 3). This indicates the probable eastward extent of the pyroxene skarn in that area before the retrograde phase of main skarn.

In the quarry east of Bakırlık Tepe, iron mineralization (Fig. 14) occurs as banded magnetite iron ore which intersects the garnet skarn. Magnetite bands have a thickness of 5 to 10 cm and are oriented parallel to the marble/skarn contact. About 350 tons of massive magnetite ore was extracted from this quarry. Whole rock analyses from skarns show that this skarn has a calcic character and can develop minor Fe mineralization (Fig. 13). According to experimental studies, we know that the andradite stability is restricted to fluids rich in H_2O at relatively low temperatures (i.e. below 400°C; Meinert et al. 2005; Gustafson, 1974). The decomposition of andradite to quartz+calcite+iron oxide in a fluid H_2O+CO_2 highlights a retrograde process. Indeed, in the garnet skarn andradite has a composition of Ad_{90}. Sample G-23 contains, besides a small amount of epidote, quartz, calcite, and iron oxide (magnetite and/or hematite) as the main retrograde phases (Fig. 7F; G-26c).

In the field, a small quarry operated to extract sphalerite in the middle of the pyroxene skarn, also explains the only presence of zinc in the pyroxene skarn (Fig. 3; No.6 and No.7). Samples G-22 and G-23 show abnormal Zn content (Table 3). Another proof comes from the analyses of pyroxenes which show a clear zinc enrichment (G-5; ZnO = 0.26-0.41%). Such pyroxenes coincide with the metasomatic pyroxenes which contain a large amount of Fe^{2+}, which has similar cationic size and electronegativity to those of zinc. On the triangular diagram, these pyroxenes are perfectly correlated with the field of lead-zinc deposits (Fig. 15).

Figure 14. Garnet skarn with magnetite bands.

The "hydrated" endoskarn shows a Zn-affinity expressed by manganese minerals (epidote, chlorite, sphalerite and bornite, Fig. 7D) and whole rock analysis (G-25; Table 3). This indicates the possibility of widespread pyroxene skarn in exoskarn before the retrograde phase.

7. EVOLUTION OF SKARN FORMATION

We envisage three stages for the formation of Ca-Mn skarn at Bakırlık Tepe (Fig. 16; steps I, II, III). These stages are described below:

Contact metamorphic stage (isochemical reactions): The intrusion of the pluton has caused a strong contact metamorphism (Fig. 16; step I), where the limestone turned into coarse grained marble and the greywacke to amphibole hornfels. The calc-silicate hornfels occurs along the marble in an area where it had probably an impure composition (crust of the marble block). The estimated conditions are: pressure between 1.5-2.0 kbar, average XCO_2 values and temperature around 550°C. Probably, at the end of this stage the marginal facies of monzonite altered to dioritic composition due to calcium assimilation.

Contact metasomatic stage (replacement of marble and formation of prograde endoskarn/exoskarn): The metasomatic activity (Fig. 16; step II) was more intense in the west of the roof pendant where the marble was completely altered to garnet and pyroxene skarns. Only, a small part of the initial phases of marble survived this alteration. The endoskarn is zoned towards the monzonite-skarn contact. The original diorite, monzodiorite alters first to hornblende-diopside monzonite and then finally to garnet endoskarn towards the monzonite-garnet skarn contact and monzogabbro towards the monzonite-pyroxene skarn contact.

Epidote endoskarn ("hydrated" endoskarn), on the other hand, was developed at the monzonite-marble contact in response to intensive fluid activity. The marble was a natural barrier, stopping fluids.

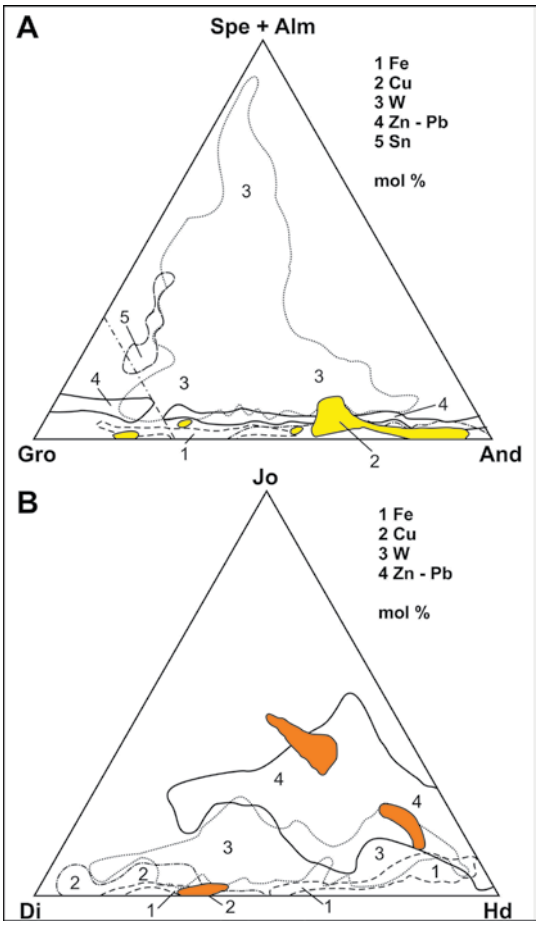

Figure 15. Garnet (A) and pyroxene (B) compositions associated with skarn ore mineralization. The dotted line at left side in the ternary diagram separates metasomatic garnets from other garnet compositions (Einaudi and Burt, 1982). Evolution of garnet and pyroxene compositions in skarn: a comparison with evolutionary diagrams from Einaudi and Burt (1982) highlights the close relationship between the silicate and ore mineral compositions of skarn deposits (Fe, Pb-Zn and Cu). Mn-pyroxenes are associated with lead-zinc skarn ore deposits.

Prograde skarn crystallization is thought to have developed under the following conditions: temperature between 400-450°C, XCO_2 of about 0.01 and a shallow intrusive emplacement (1kbar). The presence of clinozoisite+grossularite+quartz in grain interstices demonstrates a minimum temperature of 400°C. On both sides of the marble horizon the vein type skarnoid deposition is different: epidote is concentrated on the magmatic rock side, whereas grossularite was observed on the Çetmi Mélange's greywacke side.

Retrograde stage (alteration to skarn ore mineralization): The final stage is marked by the retrogression of the skarn and metalliferous mineralization (Fig. 16; step III).

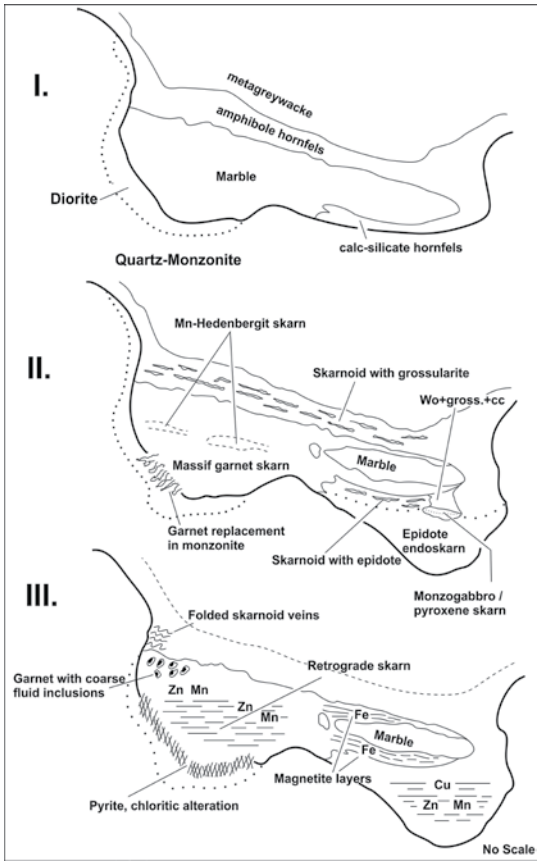

Figure 16. Evolution of skarn formation at Bakırlık Tepe (steps illustrating the probable development of the prograde skarn and hydrothermal activity). I. Contact metamorphic (isochemical) evolution, II. Metasomatic evolution (replacement, main skarn), III. Retrograde skarn evolution (late alteration of main skarn phases and endoskarn).

Mn-enrichment occurs on the periphery of the crystals. Concentrated in some places, this phenomenon does not have common origin within the marble but linked with the directions of fluid movement. Mn-skarns are closely related to Pb-Zn minerals. Silicate minerals are enriched in Fe^{2+} and Mn; this particularly concerns the clinopyroxene. The distribution of the metallic elements is very obvious: Cu and Fe in garnet skarn, Zn in pyroxene skarn. At Gürece, this type of skarn is associated with a shallow emplaced intrusion and a largely oxidized skarn environment (andradite). The substitution of hedenbergite by johannsenite suggests lower temperatures below 400°C and an increase in fO_2 and fS_2. This accompanies the precipitation of pyrite and sphalerite instead of pyrrhotite.

8. CONCLUSIONS

Typical mineralogy of manganesiferous Zn-skarn minerals occurs on Bakırlık Tepe hill, NE of Gürece, where the duality of skarn (garnet skarn + pyroxene skarn) and associated metal mineralization are exposed.

The Middle Eocene Gürece Pluton, a very homogeneous, relatively coarse grained body of hornblende quartz monzonite intrudes near Bakırlık Tepe hill the greywacke and a pile of limestone, probably an olistostrome in the Çetmi Mélange which suffered intense skarn alteration.

The endoskarn and exoskarn zones are well developed with the existence of obvious magmatic character marked by a relict granular, highly fractured texture and especially by the presence of magmatic K-feldspar. A clear endoskarn was observed at the pyroxene skarn contact and is surrounded by an epidote endoskarn (“hydrated”endoskarn).

Generally, garnet composition is intermediate in the grossularite-andradite series but in contact with the pyroxene zone, Fe and Mn are enriched. The pyroxene shows the same tendencies (Fe-diopside enriched in Mn). Some interspaces are filled by later epidote.

On Bakırlık Tepe, at contact between the Gürece monzonite and very low grade metamorphic rocks units of the Çetmi Mélange we observe a skarn evolution probably in three stages: Contact metamorphic stage (isochemical reactions), Contact metasomatic stage (replacement of marble and formation of prograde endoskarn/exoskarn) and a late retrograde stage (alteration to skarn ore mineralization). This final stage is marked by the retrogression of the skarn and metalliferous mineralization.

Currently, the Gürece contact is the only studied example of Zn-skarn in the region. The results of this study should shed light to an understanding of other outcrops of Pb-Zn minerization that we know in the Biga Peninsula and elsewhere (Pelitli, Gebze, İstanbul; Bağırkaç dere, Havran Balıkesir; Balya mine, Balıkesir; north of Domaniç, Kütahya). Formerly skarn studies in Turkey are often based on geochemistry and stability of metallic minerals. We now assume that the detailed research of skarn

silicate mineralogy and study of fluid inclusions will provide important clarifications on the relationship of silicate minerals and ore mineralization.

ACKNOWLEDGEMENT

We thank Editor Prof. Dr. Timur USTAÖMER and two anonymous referees and Dr. Francis Saupé from CRPG of Nancy (France) for their constructive comments on the manuscript.

REFERENCES

Aygül, M., Topuz, G., Okay. A.İ., Satır, M. & Meyer, H-P (2012). The Kemer Metamorphic Complex (NW Turkey): a subducted continental rim of the Sakarya Zone. Turkish J. Earth Sci., Vol.21, 19-35.

Beccaletto, I., Bonev, N., Bosch, D. & Bruguier, O. (2007). Record of a Palaegene syn-collosional extension in the north Aegean region: evidence from the Kemer micaschists (NW Turkey). Geol. Mag 144, 393-400.

Boctor, N.Z. (1985). Rhodonite solubility and thermodynamic properties of aqueous MnCl 2 in the system MnO-SiO_2 -HCl-H_2O Geochim. Cosmochim. Ac. Vol.49, 565-575.

Brennich, G. (1961). Türkiyede Demir Cevheri Zuhuratı. MTA Rapor Numarası: 3440.

Bucher, K. & Grapes, R. (2011). Petrogenesis of metamorphic rocks. Springer.8th ed., 419p.

Burt, D.M. (1972). The facies of some Ca-Fe-Si skarns in Japan. 24 th IGC Section 2, 284-288.

Burt, D.M. (1977). Mineralogy and petrology of skarn deposits. Makes. Soc. Ital. Min. Petr. Vol.33, 859-873.

Burton, J.C, Taylor, L. A & Chou I.M. (1982). The fO_2 and fS_2 T-stability relationship of hedenbergite and hedenbergite-johannsenite solid solutions. Econ. Geol. Vol.77, 764-783.

Çalapkulu, F. (1976). Geology map H17b2-b3 (in Turkish). Rap. Intern. Min. Res. Expl. Inst., Turkey. No. 6826.

Duru, M., Pehlivan, Ş., Okay, A.İ., Şentürk, Y. and Kar, H. (2012). Biga Yarımadası'nın Tersiyer Öncesi Jeolojisi, p.7-74, Biga Yarımadası'nın Genel ve Ekonomik Jeolojisi, Editörler: Erdoğan Yüzer, Gürkan Tunay, MTA Özel Yayın Serisi, No: 28, Ankara (in Turkish).

Einaudi, M. T (1982). Description of skarns associated with porphry copper plutons in Titley S. R (ed.) Advances in geology of the porphry copper deposits, SW North America. Tucson Univ. of Arizona Press, 139-184.

Einaudi, M.T., Burt D. M. (1982). Introduction-terminology, classification and composition of skarn deposits. Econ. Geol. Vol.77, 745-754.

Gamble, R. P. (1982). An experimental study of sulfidation reactions involving andradite and hedenbergite. Econ. Geol. Vol.77, 784-797.

Greenwood, H. J. (1967). Mineral equilibria in the system MgO-SiO_2-H_2O-CO_2 in P.H. Abelson (ed.) Researches in geochemistry Vol.2, 542-567.

Gulbrandsen, R.A., Gielow D.G. (1960). Mineral assemblage of a pyrometasomatic deposit near Tonopah, Nevada. US Geol.Surv. Prof. Pap. 400-B, 20.

Gustafson, W.I. (1974). Stability relationships of andradite, hedenbergite, and related minerals in the system Ca-Fe-Si-OH. Journ. Petr. Vol.15, 455-496.

Huckenholz, H.G., Yoder, H.S. (1971). Andradite stability in air at 1 atm O_2 up to 30 kb and H_2O+O_2 up to 20 kb total pressure. Ann. rep. Dir. Geophysics. Lab. Wash. 1969-1970, 182.

Kerrick, D.M. (1977). The genesis of zoned skarns in the Sierra Nevada, California. Journ. Petr. Vol.18, 144-181.

Keskin, M. (2002). Karabiga (Biga - Çanakkale) granitoyid plütonu batı kesiminin ve yan kayaçlarının petrolojisi. Y.Lisans tezi. Istanbul Üniversitesi. (M.Sci Thesis, in Turkish). 99s.

Korkmaz, A.C., Aysal, N., Ustaömer, P.A. & Peytcheva, I. (2012). U/Pb LA-ICP-MS zircon geochronology and tectonic setting of the Gürece stock (Lapseki-Çanakkale). 5th Geochemistry Symposium with international participants, 23 – 25 May 2012. Pamukkale University, Denizli, Turkey. 191.

Megaw, P. K. M., Ruiz J., Titley, S.R. (1988). High temperature, carbonate hosted Ag-Pb-Zn (Cu) deposits of northern Mexico. Econ. Geol., Vol.83, 1856-1885.

Meinert, L. D. (1984). Mineralogy and petrology of iron skarns in western British Columbia, Canada. Econ. Geol. Vol.79, 869-882.

Meinert, L.D. (1992). Skarns and skarn deposits.

Geosci. Can., Vol.19, 145-162.

Meinert., L.D., Dipple, G.M. and Nicolescu, S. (2005). World skarn deposits, Economic Geology, v. 100, pp. 299-336.

Morimoto, N. (1988). Nomenclature of pyroxenes. Bull. Miner. Vol.111, 535-550.

Okay, A.I. & Tüysüz, O. (1999). Tethyan sutures of northern Turkey. In: Durand, B., Jolivet, L., Hovarth, F. & Séranne, M. (eds), The Mediterranean Basins: Tertiary Extension within the Alpine Orogen Tethyan Sutures of Northern Turkey (pp. 475–515). Geological Society, London, Special Publications 156.

Öngen, S. (1992). Les échanges métasomatiques entre granitoïdes et encaissants particuliers (calcaires, dolomites, ultrabasites, séries manganésifères): Quelques exemples en Turquie-NO. Université de Nancy I, Faculté des Sciences Terre. Thèse d'état. 554p.

Taylor, B.E., Liu, G.J. (1978). The low temperature stability of andradite in C-O-H fluids. Am Min. Vol.63, 378-393.

Taylor, B.E., O'Neil, J.R. (1977). Stable isotope studies of metasomatic Ca-Fe-Al-Si skarns and associated metamorphic and igneous rocks, Osgood Mountains, Nevada. Cont. Min. Petr. vol.63, 1-49.

Vidale, R. (1969). Metasomatism in a chemical gradient and the formation of calc-silicate bands. Am J. Sci. Vol.267, 857-874.

Yiming, Z. (1991). Manganoan skarn formation. In Theophrastus Publications (Ed.), Skarns-their genesis and metallogeny, 165-180.

Yun, S., Einaudi, M.T. (1982). Zinc-lead skarns of the Yeonhwa-Ulchin district South Korea. Econ. Geol. Vol.77, 1013-1032.

Zharikov, V.A. (1970). Skarns. Int. Geol. Rew, Vol.12, 541-559, 619-647, 760-775.